Supplemental Material

A Polymer-Integrated Flexible Gold Nanotriangle Array for Quantitative and Nondestructive SERS Detection of Thiram on Apples

Ze-Bo Zheng[1], Xiao-Hui Sun[2], Wan-Hui Guo[2], Wen Pan[2], Fan-Li Zhang[1*] and Sheng-Hong Liu[1,2*]

[1]College of Optical and Electronic Technology, China Jiliang University, Hangzhou 310018, China

[2]Xinjiang Key Laboratory of Agro-products Quality & Safety, Institute of Quality Standards & Testing Technology for Agro-Products, Academy of Agricultural Sciences of Xinjiang Uyghur Autonomous Region, Urumqi, 830091, China

*Corresponding author email: denis.boudreau@chm.ulaval.ca and zhangfl@cjlu.edu.cn

S1. UV-vis characterization during AuNTs synthesis and purification

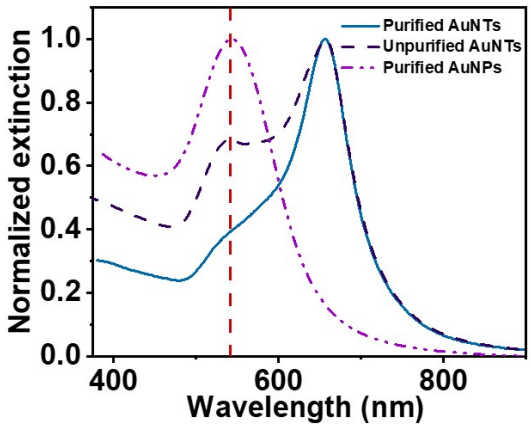

Figure. S1. UV-vis extinction spectra of AuNTs before and after purification, as well as the by-products after purification.

S2. Calculation of CTAC volume for depletion-induced purification

The volume of CTAC solution required to achieve the target final concentration during depletion-induced purification was calculated following the method reported by Scarabelli et al[1].

The required CTAC volume (V_χ) was calculated using the following equation:

$$V_\chi = \frac{V_{\text{in}}(C_{\text{fin}} - C_{\text{in}})}{C_{\text{supply}} - C_{\text{fin}}}$$

where V_{in} is the initial volume of the AuNTs growth solution, C_{in} is the initial CTAC concentration in the growth solution, C_{fin} is the desired final CTAC concentration, and C_{supply} is the concentration of the supplied CTAC stock solution (25 wt%).

Based on this calculation, the required CTAC volume added during purification

was calculated to approximately 7.15 mL.

S3. SEM characterization of AuNTs purification, assembly, and transfer

SEM images of AuNTs at different stages of purification, assembly, and transfer are shown in Figure. S2. Before purification, Au nanoparticles and AuNTs coexist. After selective purification, the AuNTs were assembled and transferred onto silicon substrates, forming densely packed and ordered arrays. Subsequently, the assembled AuNTs arrays were transferred onto BOPP films, demonstrating the successful transfer of the assembled structures onto flexible substrates.

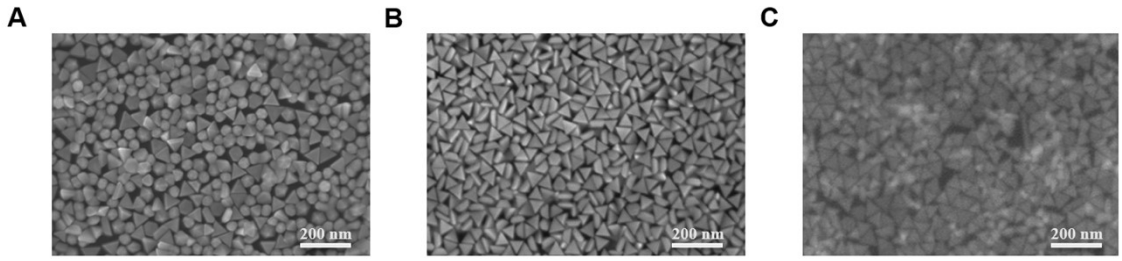

Figure. S2. SEM images of self-assembled AuNTs before purification, after purification on a silicon substrate, and after transfer onto a BOPP film.

S4. Optimization of ligand concentration and aggregating agents in self-assembled AuNTs arrays for Rh B detection

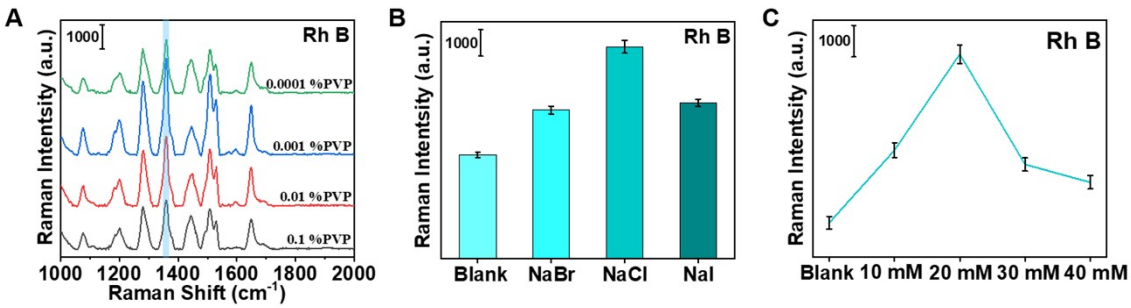

Figure. S3. Optimization of self-assembled AuNTs for RhB detection. Optimization of PVP concentration (A), aggregating agent type (B) and aggregating agent concentration (C).

S5. Calculation of the analytical enhancement factor (AEF)

The AEF of the flexible AuNTs array was estimated according to the following equation[2]:

$$AEF = \frac{I_{SERS}/C_{SERS}}{I_R/C_R}$$

where I_{SERS} and I_R represent the Raman intensities obtained under SERS and normal Raman conditions, respectively, and C_{SERS} and C_R correspond to the Rh B concentrations used for SERS and normal Raman measurements.

For the SERS measurements, Rh B aqueous solution with a concentration of $C_{SERS} = 0.1$ μg/L was drop-cast onto the optimized flexible AuNTs array substrate and dried under ambient conditions before spectral acquisition. The SERS spectrum was collected from the central region of the substrate, and the Raman intensity at 1358 cm^{-1} was recorded as $I_{SERS} = 801.2$, obtained from multiple measurements. For the normal Raman measurements, Rh B aqueous solution with a concentration of $C_R = 10$ g/L was deposited onto a silicon wafer. The Raman intensity at 1358 cm^{-1} was recorded under identical instrumental conditions, yielding an average value of $I_R = 215.4$. Based on these values, the AEF of the flexible AuNTs array was calculated to be approximately 3.72×10^8.

S6. Assignment of common raman characteristic peaks of thiram

Table S1. Common characteristic peak assignments of thiram

Raman shift	Characteristic peak assignment
386 cm^{-1}	S–S bond stretching vibration
427 cm^{-1}	CSS deformation vibration

568 cm^{-1}	S–S stretching vibration and symmetric stretching vibration of CSS
1372 cm^{-1}	symmetric bending vibration of CH_3

S7. Calculation of the Limit of Detection (LOD)

The limit of detection (LOD) was calculated using the 3σ/k method. The following steps were used to standardize the expressions for unit conversion and dilution factor to ensure consistency:

Calculation formula for the standard deviation (σ) of blank signals:

$$\sigma = \sqrt{\frac{\sum_{i=1}^{n} (I_i - \bar{I})^2}{n-1}}$$

Where I_i is the individual Raman signal intensity of blank samples, $\bar{I}$ is the average Raman signal intensity of blank samples, and n is the number of blank sample tests;

Standard curve equation of thiram: Y = 2189 X + 2498

Definition of formula parameters: k is the slope of the aforementioned standard curve;

LOD calculation results:

I_i=5.233、5.012、5.697、4.988、5.299，σ= 0.2862

LOD of thiram standard solution = 3σ/k ≈ 0.074 μg/L.

S8. The selectivity of the flexible AuNTs array

Selective detection of five common pesticides using flexible AuNTs arrays[3-6].

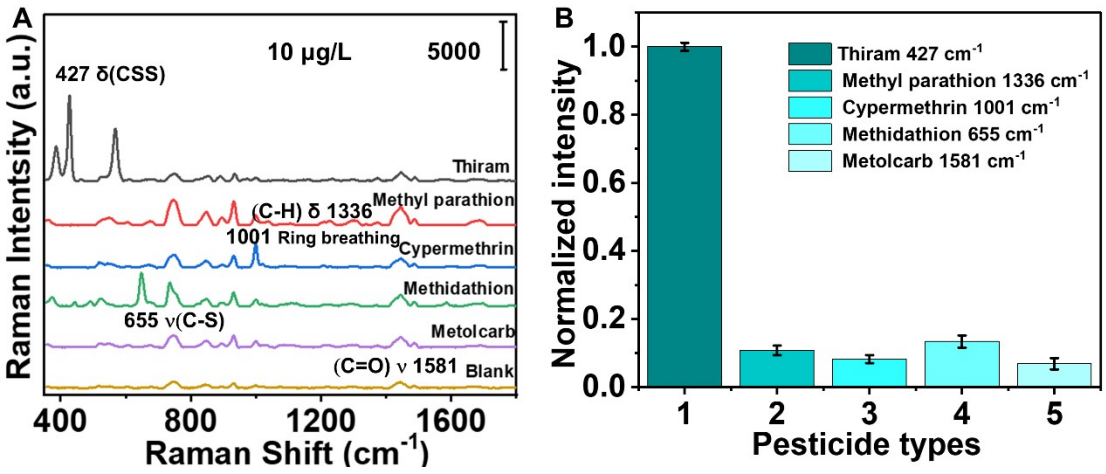

Figure. S4. (A) SERS detection of pesticides (thiram, methyl parathion, cypermethrin, methidathion, and metolcarb) at a concentration of 10 μg/L using flexible AuNTs arrays. (B) Bar chart showing the intensity of characteristic peaks for different pesticides.

References

1 L. Scarabelli and L. M. Liz-Marzán, An Extended Protocol for the Synthesis of Monodisperse Gold Nanotriangles, ACS Nano, 2021, 15, 18600-18607.

2 E. C. Le Ru, E. Blackie, M. Meyer and P. G. Etchegoin, Surface Enhanced Raman Scattering Enhancement Factors: A Comprehensive Study, The Journal of Physical Chemistry C, 2007, 111, 13794-13803.

3 J. Xie, L. Li, I. M. Khan, Z. Wang and X. Ma, Flexible paper-based SERS substrate strategy for rapid detection of methyl parathion on the surface of fruit, Spectrochimica Acta Part A: Molecular and Biomolecular Spectroscopy, 2020, 231.

4 W. Leung, S. Limwichean, N. Nuntawong, P. Eiamchai, S. Kalasung, O.-U. Nimittrakoolchai and N. Houngkamhang, Rapid Detection of Cypermethrin by Using Surface-Enhanced Raman Scattering Technique, Key Engineering Materials, 2020, 853, 102-106.

5 X.-X. Huang, Y.-C. Fan, S.-L. Chen, X.-J. Chen, S. Ali, X. Chen, L.-M. Yuan, W.

Shi, C.-X. Jiang and G.-Z. Huang, A novel SERS-based rapid and sensitive assay for methidathion detection in various fruits, Chinese Journal of Analytical Chemistry, 2022, 50.

6 Y. Wang, M. Wang, X. Sun, G. Shi, W. Ma and L. Ren, Rapid, simple and quantitative detection of metolcarb residues in apples by surface-enhanced Raman scattering, AIP Advances, 2018, 8.